Self-trapped excitons in pure and Na- and Tl-doped caesium halides and the recombination luminescence

1999 J. Phys.: Condens. Matter 11 5517

(http://iopscience.iop.org/0953-8984/11/28/312)

J. Phys.: Condens. Matter **11** (1999) 5517–5532. Printed in the UK PII: S0953-8984(99)02254-7

Self-trapped excitons in pure and Na- and Tl-doped caesium halides and the recombination luminescence

Chun-Rong Fu†, Ling-Fu Chen‡ and K S Song‡

† Physics Department, University of Ottawa, Ottawa, Canada K1N 6N5

‡ Physics Department, Nanjing Normal University, Nanjing, People's Republic of China

Received 3 March 1999, in final form 24 May 1999

Abstract. On the basis of a method used earlier to predict the off-centre relaxed triplet self-trapped excitons in alkali halides, similar systems in caesium halides are studied. This work confirms the expected off-centre relaxation along the [100] cubic axes with increasing magnitude in the order CsI, CsBr and CsCl. The calculated emission energies are in reasonable agreement with observed values. The well-known 2.95 eV emission band of CsI:Na has been studied as a tunnelling recombination between a close pair consisting of a V_K centre and a Na atom. For a number of close-pair geometries the emission energies are close to 3 eV. The strong emission bands of CsI:Tl at 2.25 eV and 2.55 eV have been interpreted as arising from tunnelling recombination of close pairs each consisting of a Tl^0 and a V_K centre. The calculated emission energies and polarizations are discussed in conjunction with the experimental data.

1. Introduction

The photoluminescence of pure and activator-doped caesium halides, in particular that of CsI, has been extensively studied. CsI and CsI:Tl are some of the best-known scintillating materials [1]. Recent experimental studies have indicated that some of the emission bands are of excitonic origin, in particular those of the spin-triplet self-trapped excitons (STE) which are similar to those of alkali halides with the NaCl lattice [2,3]. Beside the studies of luminescence, the following investigations have been reported, among others: optically detected magnetic resonance (ODMR) studies of CsBr [4] and CsI [5]; and transient absorption studies, which explore higher bound states of the self-trapped exciton [6]. On the basis of these studies and from comparison with alkali halides of NaCl structure, it has been generally accepted that the STE is of the off-centre type in which the excited electron and the self-trapped hole are split in space, presumably along the anion row (100) in the CsCl lattice [6].

As for the caesium halides doped with Na and Tl, the luminescence bands are not only different in energy and lifetime from the intrinsic ones, but they are also more complex. The 2.95 eV band for CsI:Na has been attributed to tunnelling recombination of the Na-bound electron with the V_K centre at low temperature and to thermally activated V_K centres recombining with Na centres [7]. The Tl centre produces more complex bands. The two UV bands are attributed to intra-Tl transitions associated with lattice distortion of lowered symmetry [2, 3]. On the other hand, the two visible-light bands are considered to originate from the Tl-perturbed STEs, which exhibit stronger off-centre relaxation than in the pure host [2, 3].

In this paper we report the results of a calculation on the structure of the STE in CsCl, CsBr and CsI. We have also studied several possible models of recombination in CsI doped with Na

0953-8984/99/285517+16$30.00

and Tl in order to achieve an understanding of the origins of the strong emission bands. The method used is the same as in our earlier studies which predicted the off-centre relaxation of the triplet STE and the relationship between the off-centre relaxation and F-centre formation in alkali halides of NaCl structure [8]. In this approach the excited electron is treated within the one-electron Hartree–Fock approach by orthogonalizing the electron wavefunction to all of the occupied orbitals of the surrounding ions. While the atom–atom interaction is described by classical pair potentials, the self-trapped hole is separately treated using a CNDO (complete neglect of differential overlap) code. In determining the equilibrium structure of the STE, the total energy is minimized by searching for the optimum atomic positions which correspond to zero energy gradient.

The main points of the results obtained are as follows.

(a) The triplet STE in each of the three caesium halides is off-centre relaxed along the anion row (100), with increasing off-centre shift in the order CsI, CsBr and CsCl. The estimated emission energies are in reasonable agreement with experimental values.
(b) The absorption energies to the electron excited states of the off-centre STE are in good agreement with the data of Itoh *et al* [6] and rather insensitive to the exact magnitude of the off-centre shift.
(c) In CsI, the on-centre STE energy is lower than some of the off-centre values and this suggests that the on-centre STE might be metastable.
(d) The tunnelling recombination energy of the close-Na-and-V_K centre is in good agreement with the observed value of 2.95 eV.
(e) Studies of the Tl-perturbed STE in CsI have not produced emission band energies comparable with those from experiment (2.55 eV and 2.25 eV). On the other hand, the recombination of Tl-bound electrons with the nearby V_K centres has yielded interesting results.

On the basis of this work and other experimental observations, we propose that the strong visible bands are the result of tunnelling recombination of the Tl-trapped 6p electrons and the nearby V_K centres.

This paper is organized as follows. In section 2 we describe the main elements of the method used. In section 3 the results obtained are presented and discussed in relation to the available experimental data.

2. Method of calculation

The method follows closely the one used in our previous studies of the STEs in alkali halides with NaCl lattices [8,9], but has a more efficient routine for the energy minimization. A single electron (or two electrons as in positronium [10], for example) is represented within the one-electron Hartree–Fock approach. All other occupied electrons are considered to be frozen, as in the perfect crystal. The atom–atom interaction is described by classical pair potentials of Buckingham type which have been fitted to the crystal properties. Because of the presence of the hole centre, which undergoes a large relaxation accompanied by hole diffusion, a separate CNDO code has been interfaced. Our earlier studies based on the present approach have been followed recently by *ab initio* many-electron Hartree–Fock calculations for several alkali halides, and these confirmed the main features derived for the STE [11, 12]. In view of there being heavier ions involved in the present system, a similar all-electron *ab initio* calculation would require even larger resources. In the following, we present the main aspects of the method used as well as the parameters employed. More details can be found in various earlier publications [8, 9, 13, 14].

2.1. Ion–ion pair interaction

The ions in the crystal are assumed to have their nominal charges: Cs: +1 and X: −1, where X stands for the halogen atoms. This is also the case for the substitutional dopants Na and Tl. Lattice Coulomb energy changes contributed by displaced ions are evaluated by using the cubic harmonics expansion of the Madelung potential of an infinite point-charge lattice up to order 10. The short-range inter-ionic pair potentials used are of Buckingham type; and these were fitted earlier for use in shell-model studies [15] and are taken to be acting between nearest neighbours of the corresponding ion pairs. Their values are shown in table 1. For the impurity Na and the nearest anion, we have used the values for the corresponding host crystals NaX. For the Tl and anion interaction, we have evaluated the repulsive interaction using the electron gas model of Gordon and Kim [16]. The parameters used are also in table 1.

Table 1. Parameters of the pair potentials: $V(r) = A\mathrm{e}^{-r/\rho} - C/r^6 - D/r^8$ (all in atomic units).

Coeff-icient	Cs^+–Cs^+	Cs^+–Cl^-	Cl^-–Cl^-	Cs^+–Br^-	Br^-–Br^-	Cs^+–I^-	I^-–I^-	Na^+–I^-	Tl^-–I^-
A	1.317×10^{15}	173.3452	123.5135	162.1735	100.8761	180.5480	93.0486	28.9987	334.40
ρ	0.1593	0.65278	0.6735	0.6886	0.7532	0.7207	0.8454	0.7235	0.5829
C	402.1175	342.3537	424.4513	537.4279	761.1020	803.1977	1698.6511	86.6509	—
D	1029.0139	1286.2674	1607.8044	1029.1039	3156.8215	2688.9142	7026.6164	259.2250	—

2.2. Excited electron treatment

In the present system a single electron is treated in the Hartree–Fock equation. The basis function is composed of floating Gaussians centred at suitable positions in space.

The Hamiltonian of the system is given as

$$H = -\frac{1}{2}\Delta^2 + V_{pi}(\vec{r}) + V_{sc}(\vec{r}) + V_{ex}(\vec{r}) \tag{1}$$

where V_{pi}, V_{sc} and V_{ex} are the point-ion potential, screened Coulomb potential and exchange potential, respectively.

The defect electron wavefunction is represented by Ψ, which is orthogonal to all of the ionic orbitals $\chi_{\gamma,\lambda}$ ($\chi_{\gamma,\lambda}$ is the λth occupied atomic orbital on the γth atom):

$$|\Psi\rangle = \sum_i c_i \left(|\phi_i\rangle - \sum_{\gamma,\lambda} |\chi_{\gamma,\lambda}\rangle\langle\chi_{\gamma,\lambda}|\phi_i\rangle \right) \tag{2}$$

where ϕ_i is a floating 1s Gaussian ($\exp(-\alpha_i(\vec{r} - \vec{R}_i)^2)$). Either Gaussians at different positions or different Gaussians at the same position are used in the linear combination. The problem now is solving the secular equation for the state Ψ and its energy E:

$$|H_{i,j} - E S_{i,j}| = 0. \tag{3}$$

In the course of atomic relaxation toward an equilibrium configuration, the matrix elements H and S are evaluated a great number of times. They include a number of short-range energy terms as well as the overlap integrals involving the Gaussian basis and the various core and valence orbitals of the ions. While for the valence electron shells, they are evaluated by means of convenient interpolation formulae, the deeper core electrons are represented by the so-called 'ion-size' parameters [13]. Details are given in appendix A.

The occupied Cs orbitals are those given in reference [17], and the anion orbitals have been recalculated to take into account the compression of the valence shells in an attractive Madelung

potential of the ionic lattice. Furthermore, we have made the usual approximation that the ionic core energy is merely shifted from the free-ion energy by the appropriate Madelung potential:

$$H|\chi_\lambda\rangle = (E_\lambda^0 + \Delta V)|\chi_\lambda\rangle. \tag{4}$$

It has also been assumed that ionic cores of neighbouring ions do not overlap. Although the outermost halogen p orbital shrinks substantially in an ionic lattice, this approximation is a crude one. In fact, for the Tl centre in CsI we have relaxed this simplification and included the overlap with the nearest shells of I and Cs.

The interaction of the excited electron and the halogen atom on which the self-trapped hole (STH) is localized requires a special treatment. The STH is described by a CNDO code as explained below. The long-range Coulomb interaction between the hole and the excited electron is the most important. The Mulliken population of the CNDO code was used for this term at each step of the lattice relaxation. The more subtle change of the short-range interaction terms of the Hamiltonian acting on the excited electron is treated approximately as follows.

Instead of using the molecular orbitals (MO) obtained in the CNDO code directly and orthogonalizing the floating Gaussians to them, we have represented the molecule as made up of ions and we treat them in the same way as the other ions. This was partly for the ease of computation, but also because of the crude nature of the MOs used in the CNDO code. The largest contribution from the hole centre to the excited electron energy is the long-range Coulomb interaction. This is taken care of by using the Mulliken population of the CNDO code to represent the fractional charges which change as the hole centre relaxes along the (100) axis. The short-range interaction terms have been approximated as either those from a neutral atom X^0 or those from a negative ion X^-, depending on the charge found on a given CNDO code ion. A cut-off value of $q_{cut} = 0.55$ was used such that, for $|q| \leqslant 0.55$, X was taken as X^0, and otherwise it was taken as X^- for the purpose of calculating the matrix elements of equation (A.1) in appendix A. On examining other values of the cut-off q_{cut}, we found that the result was not sensitive to the value used.

2.3. CNDO representation of the hole

The hole centre is represented by the CNDO code. While all other ions are considered to be frozen in their perfect-lattice states, the several (in the present work four) halogen atoms on which the self-trapped hole (the V_K centre) is localized and along which it is hopping have to be treated specially. Most important is that the hole population changes and that the covalent bond which keeps the hole localized on a pair of halogens until the hole jumps to the next site should be updated as the system relaxes in the lattice. The CNDO parameters have been refitted to the following known data for the halogen molecule ions calculated in reference [18]: the equilibrium bond length, the stretching mode vibrational frequency and the dissociation energy. The values of the parameters used are given in table 2.

Table 2. CNDO parameters.

Ion	I_s	I_p	β	α
Cl^-	−19.1	−6.95	−7.8	1.90
Br^-	−25.2	−6.37	−6.9	2.20
I^-	−19.1	−5.67	−5.6	2.33

2.4. Relaxation of the lattice

In our previous work on excited defect calculations [8, 9, 14, 19], we have optimized the positions of several dozens of atoms by evaluating the energy gradient and determining the local energy minimum one atom at a time. This sequence was repeated a number of times until the total energy of the system reached a predetermined threshold of convergence. In the present work, we improved the minimization routine by relaxing groups of atoms by symmetry. Energy gradients **G** for all atoms were evaluated before moving any atoms. Then the energy surface was fitted to a quadratic form $E(\alpha)$ and all atoms were displaced to the new positions **X** in the following way.

The quadratic form $E(\alpha)$ is cast in terms of a non-negative variable α, which determines the displacement of the whole system along the direction of the energy gradients **G**:

$$E(\alpha) = E_0 + \alpha E_1 + \alpha(\alpha - \alpha_1)E_2 \tag{5}$$

which interpolates between $E(\alpha)$ at $\alpha = 0, \alpha_1$ and α_2.

On setting $\mathrm{d}E/\mathrm{d}\alpha = 0$, we obtain

$$\alpha_{min} = \frac{1}{2}(\alpha_1 - E_1/E_2). \tag{6}$$

From this, E_1 and E_2 are expressed as

$$E_1 = \frac{E(\alpha_1) - E_0}{\alpha_1} \qquad E_2 = \frac{E(\alpha_2) - E_0 - \alpha_2 E_1}{\alpha_2(\alpha_2 - \alpha_1)} \tag{7}$$

where $E(\alpha_1)$ and $E(\alpha_2)$ are the energies of the system at two different positions along the energy gradient and E_0 is the system energy for atoms at positions $\mathbf{X}_0$. Finally, the matrix **X** ($3 \times N$; N is the number of moving atoms) representing the new positions of relaxing atoms is determined as follows:

$$\mathbf{X} = \mathbf{X}_0 - \alpha_{min}\mathbf{G}. \tag{8}$$

The cycle was repeated until the largest energy gradient and the energy change both became smaller than a preset value (e.g., 0.01 eV/Bohr radius and 0.01 eV respectively). This approach leads to an improved symmetry of the atomic displacement around the defect and also resulted in a shorter computing time being required to reach the equilibrium geometry. The number of atoms explicitly relaxed varied between about 40 and 60 depending on the system studied.

In obtaining the adiabatic potential energy surface (APES) relative to some configuration coordinates, we have kept a designated atom (for example, the M1 halogen atom of figure 1)

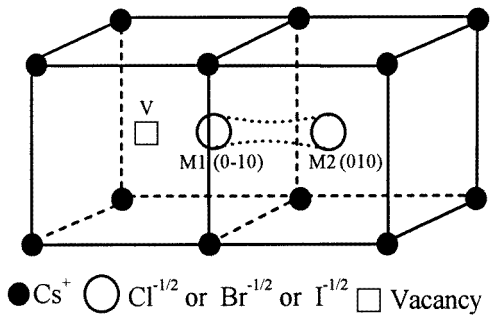

Figure 1. The lattice structure of the caesium halides. M1 and M2 denote the molecular halide ions.

at discrete steps along the (010) axis and optimized the positions of all of the other ions. When this atom reached the next halogen site, the M2 site of figure 1, the sequence was repeated by keeping the M2 ion for several steps, and so on. In this way it is possible to follow the evolution of the hole centre as it undergoes a sequence of hopping diffusion steps. The APES obtained would show whether the process is driven by a downhill energy gradient or encounters a potential barrier. The configuration coordinate chosen here, designated Q_2, represents the distance between the anion vacancy created, site V1, and the centre of gravity of the hole distribution.

3. Results and discussion

3.1. STEs in pure caesium halides and the triplet emission bands

For each of the caesium halides, we have determined the energies of a STE in the on-centre geometry (D_{4h} symmetry) and of an off-centre STE with the coordinate Q_2 over an extended range, up to about the second-nearest Frenkel defect pair (vacancy–interstitial pair). For the on-centre STE, four floating Gaussians ($\alpha = 0.005$, 0.010, 0.020, 0.030 in units of (Bohr radius)$^{-2}$, as defined in section 2.2) are placed at the mid-point between the halides M1 and M2; see figure 1. A total of 45 ions are allowed to relax. At the end of the relaxation, the hole is almost exclusively shared equally by the two central ions. This on-centre energy is indicated in figure 2 by asterisks. This energy will be compared with those of the off-centre STE later. As in our earlier work, the on-centre STE has a relatively diffuse excited electron.

The APES of the spin-triplet STE was determined as described in section 2. Two different optimized sets of three ($\alpha = 0.01$, 0.02, 0.045) or four floating Gaussian bases placed at the anion vacancy site at V1 have been used. In preliminary work we found that a Gaussian with $\alpha = 0.03$ is the optimized basis once the V_K centre has moved away, leaving an anion vacancy. Also, the electron was found to be in a diffuse orbital when in the on-centre geometry. To allow an optimum transition between the two situations, we have used basis sets comprising those Gaussians as well as some intermediate values of α.

The results obtained with the two basis sets are quite similar. In figure 2 we show those obtained with four bases ($\alpha = 0.005$, 0.010, 0.020, 0.030). The atom M1 is moved a discrete number of steps along the (010) axis until it approaches the M2 site, at which point the M2 atom which has in the meantime moved away some distance along the axis takes over the next sequence of steps. The configurational coordinate used, Q_2, in figure 2 represents (in Å) the distance between the site V1 at which the excited electron is localized and the centre of the hole population. It represents the approximate distance that the hole has slipped away from its initial position. From the above description, it is clear that Q_2 does not represent the motion of any particular atom. Any given halogen atom can travel by at most about the normal anion–anion distance in the lattice.

In order to estimate the recombination luminescence energy, the Franck–Condon ground-state energies at each of the points of figure 2 are determined. This was done, as in earlier work [9], by removing the excited electron and changing the CNDO population to the recombined configuration. The results obtained are summarized below.

(a) In all caesium halides studied, there is a clear axial instability of the triplet STE, and the equilibrium configuration is of the off-centre type. Although it is not possible to predict the precise position at which the equilibrium is reached on the APES, there is a reasonable trend of decreasing off-centre shift from CsCl to CsI. This is similar to the situation for halides of NaCl structure. As for those materials, the APES is quite flat once Q_2 has reached a certain value.

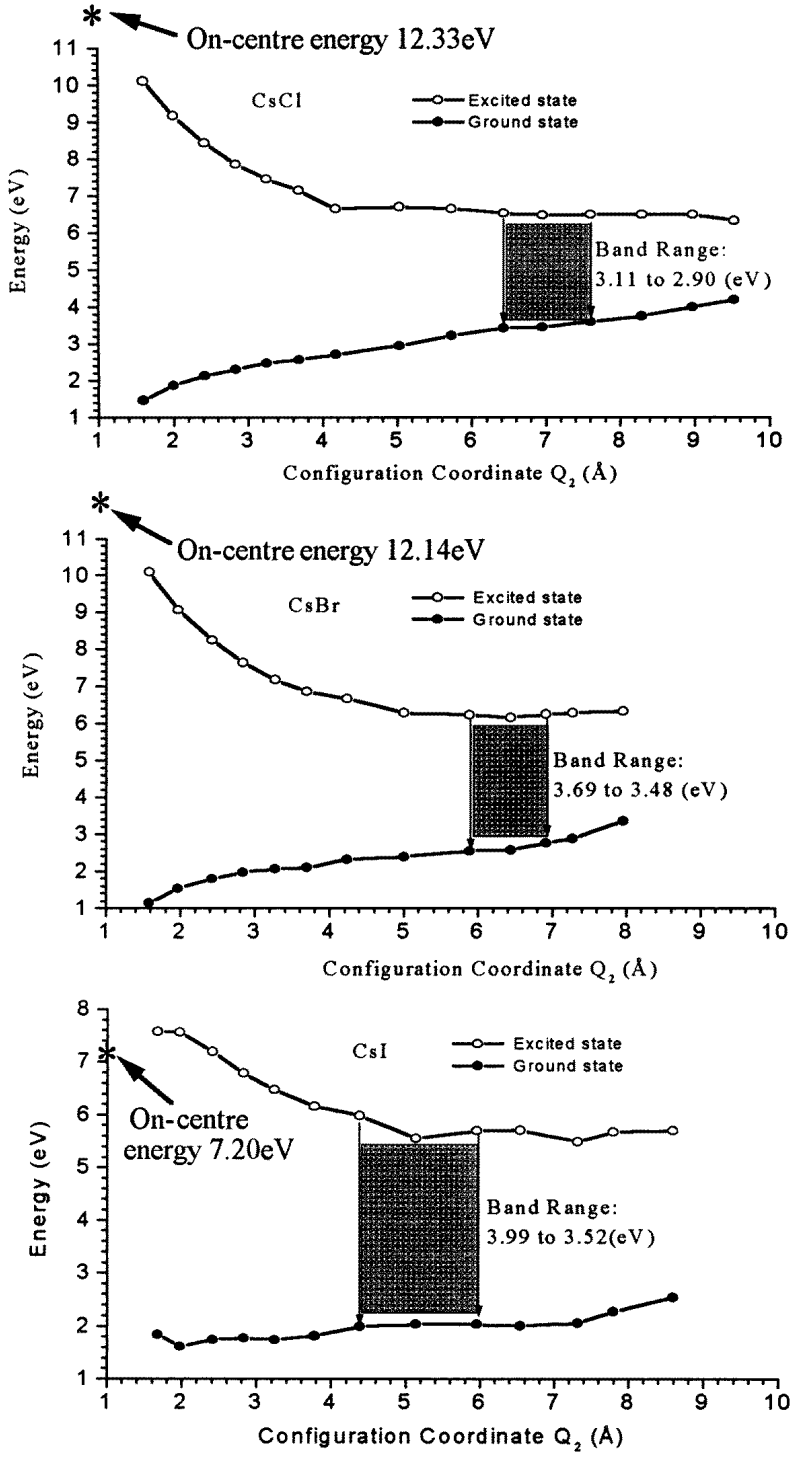

Figure 2. The APES curves of caesium halides with respect to the configuration coordinate Q_2.

In earlier work on halides with the NaCl lattice, a correlation was established between strong off-centre relaxation and the low-temperature F-centre creation yield. It is interesting to note here that for CsCl and CsBr, similar dynamic radiation damage creation at low temperature can be suggested. F-centre formation at liquid N temperature in CsBr has been studied by Saidoh and Itoh [20].

(b) A new aspect for the caesium halides is that the energy of the on-centre STE is closer to the off-centre energies, especially for CsI. For this latter, the calculated on-centre energy is lower than the off-centre one for small values of Q_2. It could be that the on-centre STE is metastable, separated from the more stable off-centre STE by a potential barrier. We will come back to this point later.

(c) We have indicated in figure 2 the range of Q_2 over which radiative transition to the ground state could take place. The calculated emission energies are in acceptable agreement with the experimental values when the approximate nature of the method used and the flatness of the APES near equilibrium are taken into consideration. From our work, the ground-state APES rises more steeply for CsCl than for the other compounds near the equilibrium Q_2. This can be compared with the larger emission bandwidth of CsCl (0.7 eV) compared with other compounds (0.28 eV and 0.51 eV respectively for CsBr and CsI [3]). The 4.3 eV band in CsI has been attributed to the on-centre STE [2, 21, 22]. It has also been reported that this band and the main 3.7 eV band are connected by thermally exchanging intensity. Our calculated emission energy for the on-centre STE, possibly a metastable state, is about 5 eV. If this is indeed related to the on-centre STE, this may be an interesting case to explore further.

(d) Lower-energy transient absorptions are attributed to the electron excited states of p-like orbitals. For CsCl and CsBr these bands are at 1.74 and 1.19 eV respectively [6]. We have calculated the lower p-like excited states at several values of Q_2 near equilibrium. Using optimized sets of four Gaussians (arranged along the x-axis) to simulate the p_x state ($\alpha = 0.010$ at ± 0.20; 0.025 at ± 0.40; 0.035 at ± 0.55; 0.045 at ± 0.05 for CsCl and 0.010 at ± 0.10; 0.025 at ± 0.60; 0.030 at ± 0.50; 0.038 at ± 0.050 for CsBr) we obtained absorption energies which are not very sensitive to Q_2. The calculated values are in good agreement with experiment. They are shown in table 3.

Table 3. p-like excited states and transient absorption energies at several values of Q_2 near the equilibrium.

Crystal	Q_2 (Å)	Calculated absorption energy ΔE (eV)	Experiment
CsCl	6.43	1.91	1.74
	6.96	2.06	
CsBr	5.88	1.15	1.19
	6.44	1.12	
CsI	5.14	1.13	N.A.
	5.96	1.15	

3.2. Luminescence of CsI:Na

The 420 nm (2.95 eV) emission band of CsI:Na is observed at both LHe temperature and at room temperature [7, 23]. At low temperature, where the V_K centre is immobile, the electron bound to Na tunnels out toward the V_K centre and recombines [24]. On the other hand,

the V_K centre becomes mobile at higher temperature and indeed the temperature dependence of the scintillation rise time shows thermally activated behaviour with the known V_K-centre activation energy of 0.13 eV [23]. In a free Na atom, the 3s electron has a binding energy of 5.14 eV [25]. At a cation site, the repulsive Madelung potential can raise this energy by about 5 eV. The presence of a V_K centre nearby makes this upward shift smaller. It is therefore conceivable that there is a relatively shallow bound electron at the Na site in CsI.

We have studied several geometries of the V_K centre with a Na atom at various positions. The relaxed system energies are shown in table 4 with a bound electron on the Na. An optimized set of three Gaussians is used for the Na-bound electron ($\alpha = 0.01$, 0.03 and 0.045 au). The lattice distortion energy is smaller when the V_K centre and Na impurity are close than when they are separated in the lattice. Our work indicates that when the two centres are nearest or second-nearest neighbours, the recombination energy is close to the observed value of 2.95 eV. The observed energy of 2.95 eV is the peak energy (with the bandwidths of 0.33 eV and 0.67 eV respectively at LHe and room temperatures) and the emission band contains many components corresponding to various separations and relative orientations of the two defects [7]. This band is well known for its long-living component, the afterglow of which can last hours at low temperature. In the present paper we have sampled a limited number of cases of separations. In tunnelling recombination, the predominant contribution to the emission band originates from close pairs. The distant pairs are either contributing to the long-lifetime components, or are too weak to be detected [26, 27].

Table 4. Tunnelling recombination energies of the V_K-centre-and-Na^0 system. The Na^0 are at (a, b, c) and three FGOs ($\alpha = 0.01$, 0.03, 0.045) are placed on the Na. The V_K centres are at (0, 0, 0) and (0, 2, 0).

(a, b, c):	(1, 0, 1)	(1, $\bar{2}$, 1)	(1, $\bar{4}$, 1)	(3, 0, 3)	Experiment
E_{ex} (eV)	3.45	4.03	3.79	3.79	—
E_g (eV)	0.76	0.93	1.00	0.91	—
E_{em} (eV)	2.69	3.10	2.79	2.88	2.95

We briefly discuss the tunnelling recombination in comparison with the normal STE recombination. With a shallow trap, such as in CsI:Na, the tunnelling of the bound electron occurs through the overlap of the wavefunction with the immobile hole centre. On the other hand, when the electron is ionized into the conduction band from a trap, it will be attracted to the hole centre where it then initiates the usual sequence of relaxation leading to the creation of the off-centre STE, as has been demonstrated in the pioneering work on the STE, in KCl:Tl [28] and in NaI [29]. The two types of recombination in alkali halides are well established. For example, the afterglow observed in irradiated KCl:Tl/Ag [26] is due to tunnelling recombination of the electron trapped on the Tl/Ag with the V_K centre, with peaks at 3.0 eV and 2.3 eV respectively for Tl and Ag, and the intrinsic π-emission occurs at 2.3 eV. As we described above, the two types of recombination are very different in nature. They contrast greatly as regards the polarization, quenching behaviour, emission energies etc [26].

3.3. Luminescence of Tl-doped CsI

Like pure CsI, Tl-doped CsI is one of the best-known scintillating materials. Recent work reported that of the four emission bands resulting from excitation into the Tl A band (4.3 eV), two UV bands (at 3.35 eV and 3.09 eV) are attributable to Jahn–Teller minima of the Tl atom and two visible bands (at 2.55 and 2.25 eV) to the Tl-perturbed STE [2]. Compared to the intrinsic emission band at 3.67 eV, the new STE bands are more strongly Stokes shifted and

the lifetimes are also longer compared with the case for pure CsI. First we describe briefly the results for the STE perturbed by a nearby substitutional Tl ion. For this system two basis sets are tried. The first one is identical to that used in section 3.1 for pure CsI, and the second one has an extra floating Gaussian at the Tl site ($\alpha = 0.01$ au or 0.03 au). It is found that there is very little population of excited electrons at the Tl site in the latter, irrespective of the basis used. The electron localizes at the iodine site, pushing the V_K core, as seen in section 3.1, and the Tl impurity mainly influences the defect through the ion–ion potential and electronic polarization. The resulting emission energy is smaller than that for the pure case. It ranges between 3.0 eV and 2.7 eV. After extensive study, however, we feel that it is unlikely that the off-centre shift could reach such a magnitude that the emission energy of around 2.25 eV, that of the strongest band, could result from these structures.

According to the current model [2], the process leading to the 2.25 and 2.55 eV bands is as follows. The Tl A-band exciton (4.3 eV) creates a hole which is initially in a valence state made up of iodine and Tl orbitals, and an excited electron on the Tl. The hole becomes quickly self-trapped, forming a V_K centre, while the Tl atom is nearby. The recombination which follows promptly is between this hole centre and the excited electron. We propose here that the two bands originate from tunnelling recombination of the Tl-trapped electron (in the 6p orbital) with the nearby V_K centre. There are several experimental results which point in this direction.

(a) Recent work based on ODMR [30] with the 2.25 eV band (the most intense of the four bands) indicates the presence of a V_K centre, rather than an H centre as one would expect from an off-centre STE. This V_K centre is somewhat perturbed by the presence of a nearby Tl atom. This situation is very similar to that observed in earlier ODMR work on CsI:Na [7]. Also, in both of these spin-resonance studies, the signature of the electron centre is absent.
(b) The 2.25 eV band in CsI:Tl and the 2.95 eV band in CsI:Na each have a long-lasting afterglow at low temperature.
(c) The Tl centre and the V_K centre seem to cluster together in space [30]. Our calculation for the V_K-centre–Tl system indicates that the lowest-energy configuration is realized when the Tl is on the mid-plane of the V_K centre and is at the nearest-neighbour site.

3.3.1. Recombination energy. In the free state, the binding energy of the Tl 6p electron is 6.1 eV [31]. Since the 6p orbital of the Tl atom is rather diffuse, it is probably even more extended in the ionic lattice. We found it necessary to take into account the overlap between the occupied 6s orbital of Tl and the surrounding I- and Cs-ion orbitals in evaluating the matrix **S** of equation (3). The overlaps with the eight I ions and six Cs ions are included in solving the secular equation.

Four pairs of floating Gaussians are placed on the Tl atom to represent a 6p electron along a chosen cubic axis ($\alpha = 0.005$, 0.01, 0.015, 0.025 au, placed separately at ± 0.4 along a cubic axis at the Tl site). For various Tl-and-V_K-centre configurations the results obtained are shown in table 5. It appears from this result that there are two groups of emission energies: the one at 2.2 eV is well separated from the others at lower energies. We propose that the $|p_y\rangle$ state of the Tl at the (1, 0, 1) site, on the mid-plane of the V_K centre, is the origin of the 2.55 eV band and that the others contribute to the 2.25 eV band. The latter is more intense experimentally by a factor of about two. Although our calculated energies are somewhat smaller than the experimental values, several features lead us to make the above proposition, as will be expanded upon below. Some distant pairs gave energies in the region of 2.4 eV, such as that with Tl at (3, 0, 3). However, these pairs probably do not contribute to the main

Table 5. Recombination energies of the V_K–Tl^0(6p) system.

Tl^+ position	State	E_{ex}	E_g	ΔE
(1, 0, 1)	p_y	3.62	1.41	2.2
	p_x, p_z	3.44	2.15	1.3
(1, $\bar{2}$, 1)	p_y	2.98	2.30	0.7
	p_x, p_z	3.52	1.78	1.7
(1, $\bar{4}$, 1)	p_y	3.67	2.15	1.5
	p_x, p_z	3.67	2.05	1.7
(3, 0, 3)	p_y	4.11	1.67	2.4
	p_x, p_z	4.05	1.78	2.3

bands because of the large distance. In general, tunnelling recombinations are considered to take place between close pairs [26, 27].

3.3.2. Polarization of the emission bands. The experimental data show interesting anisotropy in the emission bands when excited with linearly polarized light, with a complex temperature and excitation energy dependence [2]. In earlier works on the intrinsic STE luminescence in fcc alkali halides, the polarization has been determined with preferentially oriented V_K centres [26]. For example, the spin-triplet STE states are found to emit π-polarized bands while the singlet-state emission is σ-polarized [13]. We first investigate the triplet-state emission polarization of the three p states at different Tl centres around the V_K centre. The result is then compared with the reported anisotropy of the emission bands.

The hole is localized at the V_K centre in a σ_u molecular orbital, which is a p_y-like state (denoted by $|y\rangle$) in terms of the axes that we have chosen in figure 3. The spin-triplet state becomes dipole allowed as a result of the spin–orbit coupling in the hole state. This can be represented in the following way [13]:

$$|\sigma_u\uparrow\rangle = |y\uparrow\rangle + \alpha|x\downarrow\rangle + \beta|z\downarrow\rangle. \tag{9}$$

The dipole moment of the optical transition is thus given as

$$\begin{aligned}\langle\sigma_u\uparrow|\vec{\varepsilon}\cdot\vec{r}|\mathrm{p(Tl)}\downarrow\rangle &= \langle y\uparrow|\vec{\varepsilon}\cdot\vec{r}|\mathrm{p(Tl)}\downarrow\rangle + \alpha\langle x\downarrow|\vec{\varepsilon}\cdot\vec{r}|\mathrm{p(Tl)}\downarrow\rangle + \beta\langle z\downarrow|\vec{\varepsilon}\cdot\vec{r}|\mathrm{p(Tl)}\downarrow\rangle \\ &= \alpha\langle x|\vec{\varepsilon}\cdot\vec{r}|\mathrm{p(Tl)}\rangle + \beta\langle z|\vec{\varepsilon}\cdot\vec{r}|\mathrm{p(Tl)}\rangle. \end{aligned}\tag{10}$$

Here, $\vec{\varepsilon}$ is the electric field vector and p(Tl) is a p orbital at a Tl site. In our notation, $\langle x\downarrow|$ represents the unoccupied orbital on the hole centre, while $|\mathrm{p(Tl)}\rangle$ represents the occupied electron state of Tl^0. Only the spin-singlet terms contribute to the dipole matrix. For the argument of the group theoretical discussion, we can take the basis functions of the hole to be centred at the mid-point of the V_K centre. The excited electron on the Tl^0 is in a p-like state, but at a different site, such as that shown in figure 3. In order to examine the dipole matrix element connecting two wavefunctions centred at different points in space, we expand the more diffuse electron wavefunction about the hole centre which is taken as the origin (0, 0, 0). As we express the p state of the electron as a linear combination of pairs of 1s Gaussians along cubic axes, the multipole expansion is easily produced [13].

For example, $|\mathrm{p(Tl)}\rangle$ centred at $\vec{R}_0$ is represented by an odd-parity combination along the y-axis:

$$|p_y(\mathrm{Tl})\rangle = \sum_i c_i(G_i(\vec{r} - \vec{R}_0 + \Delta\vec{j}\,) - G_i(\vec{r} - \vec{R}_0 - \Delta\vec{j}\,)). \tag{11}$$

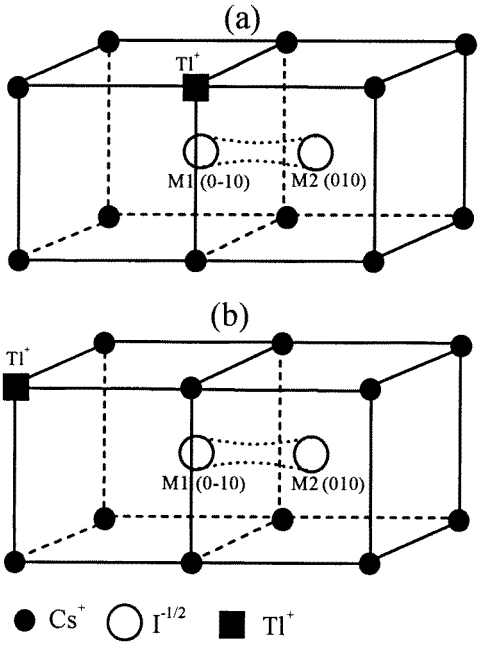

Figure 3. Configurations of caesium halide crystal doped with Tl^+. (a) Tl^+ at (1, 0, 1); (b) Tl^+ at $(1, \bar{2}, 1)$.

On the other hand, a Gaussian centred at $\vec{R}$ (e.g. $=\vec{R}_0 - \Delta\vec{j}$) can be expanded at the origin as

$$G(\vec{r} - \vec{R}) = \sum_{\ell,m} F_\ell(\vec{r}, \vec{R}) Y_\ell^m(\vec{e}_r) Y_\ell^m(\vec{e}_R). \tag{12}$$

($\vec{e}_r$ and $\vec{e}_R$ are the unit vectors along $\vec{r}$ and $\vec{R}$.) By collecting the various terms in ℓ and m, it is straightforward to determine the polarization of the dipole moment for a given Tl site and p-orbital component. To illustrate how this is done, we take the example of a $|p_y\rangle$ state of Tl at a (1, 0, 1) site (a is the cation–anion distance):

$$|p_y\rangle = G(a, -\Delta, a) - G(a, \Delta, a). \tag{13}$$

Taking the first three terms of equation (12), one finds the following results:

$$\text{for } \ell = 0: \qquad F_0[Y_0^0(\vec{e}_R) - Y_0^0(\vec{e}_R)]Y_0^0(\vec{e}_r) = 0$$

$$\text{for } \ell = 1: \qquad F_1[Y_1^y(\vec{e}_R) - Y_1^y(-\vec{e}_R)]Y_1^y(\vec{e}_r) = -\frac{2\Delta}{|\vec{R}|}F_1 y$$

however, the dipole matrix is zero for $\ell = 1$, and

$$\text{for } \ell = 2: \qquad F_2\left(\frac{2\Delta a}{R^2}\right)(yz + yx).$$

This term makes a non-zero contribution to the dipole matrix, equation (10), and its polarization vector is along the y-axis. This indicates that the $|p_y\rangle$ state of Tl at (1, 0, 1) produces a σ-polarized emission. The results collected for the two nearest-neighbour Tl sites are shown in table 6.

Table 6. Tl positions and the corresponding polarization of the emission.

Tl($\vec{R}$)	(1, 0, 1)	(1, $\bar{2}$, 1)
$\|p_y\rangle$	σ	σ, π
$\|p_x\rangle, \|p_z\rangle$	π	σ, π

From this analysis, it appears that there are two groups of emission bands with distinct recombination energies and polarizations. The higher-energy band, at 2.2 eV, is associated with the $|p_y\rangle$ state of Tl on the mid-plane of the V_K centre. The lower-energy band, below 2 eV, is associated with Tl sites at (1, $\bar{1}$, 1) of any p states. The $|p_x\rangle, |p_z\rangle$ states on the mid-plane could be part of this latter group. The first one is σ-polarized, while the second group has a mixed polarization.

This result cannot be directly compared with the observed data of reference [2]. We have made the following assumption so that the above polarization results can be compared with experiment: it is possible that the excitation into the Tl A band (at 4.3 eV) which creates the V_K centre may contribute to a partial alignment of the V_K centres; the UV absorption band for iodides is in the region of 3 eV [13]. On this assumption, then several observed features can be accounted for.

The polarization $P(\alpha)$ reported in [2] is defined as

$$P(\alpha) = \frac{I_\parallel - I_\perp}{I_\parallel + I_\perp} \tag{14}$$

where α is the angle of $\vec{E}$ for the exciting light relative to the [001] axis. The direction of observation coincides with that of the excitation beam [2, 32].

(a) By ascribing the $|p_y\rangle$ state of Tl(1, 0, 1) with the V_K centre to the 2.25 eV band, it is found that $P(0^\circ)$ and $P(90^\circ)$ are negative due to the σ-polarization (see table 6).
(b) The other bands attributed to the $|p_{x,z}\rangle$ states of Tl(1, 0, 1) and Tl(1, $\bar{1}$, 1) are more complex to analyse because of the mixed character of the polarization.
(c) The peculiar sign reversal of the polarization as the temperature is raised to 80 K could be related to the reorientation of the V_K centre. A similar variation of the polarization has been observed in the afterglow emission band for KCl:Tl(Ag) [26]. In this regard, it is interesting to note that the V_K centres in caesium halides undergo reorientation by axial diffusion (or 180° jumps), although a 90° reorientation has also been observed with higher activation energy [33]. An axial diffusion, with an activation energy of about 0.13 eV, would change the geometry of the V_K + Tl system from (1, 0, 1) to (1, $\bar{1}$, 1); see figure 3.

The tunnelling recombination considered here is similar to those observed in CsI:Na and KCl:Tl (Ag). In these examples, the prominent emission component also has a long-living afterglow. It was noted that in the ODMR of the 2.25 eV band of CsI:Tl [30] and the 2.95 eV band of CsI:Na [7], the spectra did not indicate the presence of the electron centre, while the hole centre was that of a V_K centre. These observations indicate that the two emission bands are of the same nature. We have to consider now why the ODMR spectra fit a spin Hamiltonian with spin $s = 1/2$ instead of one with $s = 1$, as is expected for a spin-triplet system. Because the distance between the hole centre and the electron centre is not large, the answer may have to be sought in the electron wavefunction. Indeed, the off-centre-STE spin-resonance spectra have all been analysed in terms of the system being a triplet [13]. For the STE the excited electron localizes strongly on the nascent anion vacancy and is rather compact, like in the F-centre ground state. This leads to a strong coupling between the hole and electron. On

the other hand, in CsI:Tl, despite the distance, which is not large, the coupling seems weak because of the relatively diffuse wavefunction of the excited electron, as we found here.

The present work, which considers the strong visible bands as originating from tunnelling recombination between the Tl atom and the nearby V_K centre, seems to be able to account for some of the observed data.

Acknowledgments

One of the authors, KSS, would like to thank M Nikl and S Zazubovich for helpful discussions.

Appendix A

The matrix elements of the Hamiltonian and the overlap integral can be expressed as follows:

$$H_{ij} = \langle\phi_i|T|\phi_j\rangle + \langle\phi_i|V_{pi}(\vec{r})|\phi_j\rangle + \langle\phi_i|V_{sc}(\vec{r}) + V_{ex}(\vec{r})|\phi_j\rangle - \sum_{\gamma,\lambda}(E^0_{\gamma,\lambda} + \Delta E_\gamma)\langle\phi_i|\chi_{\gamma,\lambda}\rangle\langle\chi_{\gamma,\lambda}|\phi_j\rangle \tag{A.1}$$

and

$$S_{ij} = \langle\phi_i|\phi_j\rangle - \sum_{\gamma,\lambda}\langle\phi_i|\chi_{\gamma,\lambda}\rangle\langle\chi_{\gamma,\lambda}|\phi_j\rangle. \tag{A.2}$$

Here we have used equation (1) and

$$\langle\chi_{\gamma',\lambda'}|\chi_{\gamma,\lambda}\rangle = \delta_{\gamma\gamma'}\delta_{\lambda\lambda'} \tag{A.3}$$

as well as

$$H|\chi_{\gamma,\lambda}\rangle = E_{\gamma,\lambda}|\chi_{\gamma,\lambda}\rangle = (E^0_{\gamma,\lambda} + \Delta E_\gamma)|\chi_{\gamma,\lambda}\rangle. \tag{A.4}$$

Equation (A.3) and equation (A.4) are based on the approximation that there is no overlap between cores of different ions. Here $E_{\gamma,\lambda}$ is the energy of the λth core orbital on the γth atom. It is the free-atomic core energy $E^0_{\gamma,\lambda}$ (e.g. taken from the Clementi and Roetti table [17]), shifted by the point-ion potential produced by the rest of the lattice, ΔE_γ.

After some manipulation, the first- and second-order ion-size terms can be expressed as

$$\sum_{\gamma,\lambda}\langle\phi_i|\chi_{\gamma,\lambda}\rangle\langle\chi_{\gamma,\lambda}|\phi_j\rangle = \sum_\gamma(f_1B_\gamma + f_2K'_\gamma + f_3K_\gamma) \tag{A.5}$$

and

$$\langle\phi_i|V_{sc}(\vec{r}) + V_{ex}(\vec{r})|\phi_j\rangle - \sum_{\gamma,\lambda}(E^0_{\gamma,\lambda} + \Delta E_\gamma)\langle\phi_i|\chi_{\gamma,\lambda}\rangle\langle\chi_{\gamma,\lambda}|\phi_j\rangle = \sum_\gamma(f_1A_\gamma + f_2J'_\gamma + f_3J_\gamma) + \sum_\gamma \Delta E_\gamma(f_1B_\gamma + f_2K'_\gamma + f_3K_\gamma). \tag{A.6}$$

The A, B, J, J', K, K' are the so-called ion-size parameters, which are calculated from deep core orbitals of free ions (the summation over λ in equations (A.5) and (A.6) is restricted to deep core shells only), while the outermost shells are treated by interpolation. The f_1, f_2 and f_3 are expansion terms of the Gaussian ϕ; they are functions depending only on the Gaussians and the vector joining them to the ion site.

The interpolation formulae for the screened Coulomb, exchange potential and overlap integrals fitted to exact values are

$$\langle\phi_i|V_{sc,\gamma}(\vec{r})|\phi_j\rangle = \int \phi_i^*(\vec{r})\frac{A_{sc,\gamma}\mathrm{e}^{-\beta_{sc,\gamma}|\vec{r}-\vec{R}_\gamma|^2}}{|\vec{r}-\vec{R}_\gamma|}\phi_j(\vec{r})\,\mathrm{d}\tau \tag{A.7}$$

$$\langle\phi_i|V_{ex,\gamma}(\vec{r})|\phi_j\rangle = \int \phi_i^* A_{ex,\gamma}\mathrm{e}^{-\beta_{sc,\gamma}|\vec{r}-\vec{R}_\gamma|^2}\,\mathrm{d}\tau. \tag{A.8}$$

It was found that two Gaussians with their exponents related in a simple ratio could give overlap integral fits of sufficient accuracy:

$$\langle\phi_i|\chi_x\rangle = N^x\int \phi_i^*(N_1^x\mathrm{e}^{-\beta_{xovl}r^2} + A_{xovl}N_2^x\mathrm{e}^{-\beta_{xovl}r^2/\kappa_x})\,\mathrm{d}\tau. \tag{A.9}$$

Here x denotes the s, p, d orbitals; κ_x is the ratio of the exponents of the two fitted Gaussians, which is determined together with A_{xovl} and β_{xovl} by the least-squares fitting procedure. N_1^x, N_2^x and N^x are normalization factors. All of the parameters used in this work can be obtained from the authors upon request.

References

[1] Rodnyi P A 1997 *Physical Processes in Inorganic Scintillators* (Cleveland, OH: Chemical Rubber Company Press)
[2] Nagirnyi V, Stolovich A, Zazubovich S, Zepelin V, Mihokova E, Nikl M, Pazzi G P and Salvini L 1995 *J. Phys.: Condens. Matter* **7** 3637
Nagirnyi V, Zazubovich S, Zepelin V, Nikl M and Pazzi G P 1994 *Chem. Phys. Lett.* **227** 1533
[3] Mihokova E, Nagirnyi V, Nikl M, Stolovich A, Pazzi G P, Zazubovich S and Zepelin V 1996 *J. Phys.: Condens. Matter* **8** 4301
[4] Marrone M J, Patten F W and Kabler M N 1973 *Phys. Rev. Lett.* **31** 47
[5] Mori Y 1989 *Radiat. Eff. Defects Solids* **108** 107
[6] Itoh M, Tanimura K and Itoh N 1993 *J. Phys. Soc. Japan* **62** 2903
[7] von der Weid J P and Aegerter M A 1978 *Solid State Commun.* **27** 519
[8] Brunet G, Leung C H and Song K S 1985 *Solid State Commun.* **53** 607
Song K S, Leung C H and Williams R T 1989 *J. Phys.: Condens. Matter* **1** 683
[9] Song K S and Leung C H 1989 *J. Phys.: Condens. Matter* **1** 8425
[10] Baetzold and Song K S 1991 *J. Phys.: Condens. Matter* **3** 2499
[11] Shluger A L, Itoh N, Puchin V E and Heifets E N 1991 *Phys. Rev.* B **44** 1499
[12] Song K S and Baetzold 1992 *Phys. Rev.* B **46** 1960
[13] Song K S and Williams R T 1996 *Self-Trapped Excitons (Springer Series in Solid State Sciences 105)* 2nd edn (Heidelberg: Springer)
[14] Fu Chun-Rong and Song K S 1999 *Phys. Rev.* B **59** 2529
[15] Sangster M J L and Atwood R M 1978 *J. Phys. C: Solid State Phys.* **11** 1541
[16] Gordon R G and Kim Y S 1972 *J. Chem. Phys.* **56** 3122
[17] Clementi E and Roetti C 1974 *At. Data Nuclear Data Tables* **14** 177
[18] Tasker P, Balint-Kurti G G and Dixon R N 1976 *Mol. Phys.* **32** 1651
[19] Fu Chun-Rong and Song K S 1997 *J. Phys.: Condens. Matter* **9** 9785
[20] Saidoh M and Itoh N 1975 *Phys. Status Solidi* b **72** 709
[21] Pellaux J P, Iida T, Nakaoka Y, von der Weid J P and Aegerter M A 1980 *J. Phys. C: Solid State Phys.* **13** 1009
[22] Tsujimoto T, Nishimura H, Nakayama M, Kurisu H and Komatsu T 1994 *J. Lumin.* **60+61** 798
[23] Kayal A H, Mori Y, Jaccard C and Rossel J 1980 *Solid State Commun.* **35** 457
[24] Ong C K, Song K S, Monnier R and Stoneham A M 1979 *J. Phys. C: Solid State Phys.* **12** 4641
[25] Moore C E 1971 *Atomic Energy Levels* NBS Circular No 467, vol 1 (Washington, DC: US Government Printing Office) (reissued)
[26] Delbecq C J, Toyozawa Y and Yuster P H 1974 *Phys. Rev.* B **9** 4497
[27] Williams R T, Williams J W, Turner T J and Lee K H 1979 *Phys. Rev.* B **20** 1687
[28] Kabler M N 1964 *Phys. Rev.* **136** A1296
[29] Murray R B and Keller F J 1965 *Phys. Rev.* **137** A942

[30] Spaeth J-M, Meise W and Song K S 1994 *J. Phys.: Condens. Matter* **6** 3999
[31] Moore C E 1971 *Atomic Energy Levels* NBS Circular No 467, vol 3 (Washington, DC: US Government Printing office) (reissued)
[32] Zazubovich S 1994 *Int. J. Mod. Phys.* B **8** 985
[33] Monnier R, Song K S and Stoneham A M 1977 *J. Phys. C: Solid State Phys.* **10** 4441